An Oversampling Technique for Multiscale Finite Volume Method to Simulate Frequency-domain Electromagnetic Responses

*L. A. Caudillo-Mata**, E. Haber, and C. Schwarzbach*
Geophysical Inversion Facility, Earth, Ocean and Atmospheric Sciences Department, University of British Columbia
4013-2207 Main Mall, Vancouver, British Columbia, Canada, V6T 1Z4

SUMMARY

To reduce the computational cost of the simulation of electromagnetic responses in geophysical settings that involve highly heterogeneous media, we develop a multiscale finite volume method with oversampling for the quasi-static Maxwells equations in the frequency domain. We assume a coarse mesh nested into a fine mesh, which accurately discretizes the setting. For each coarse cell, we independently solve a local version of the original Maxwell's system subject to linear boundary conditions on an extended domain, which includes the coarse cell and a neighborhood of fine cells around it. The local Maxwell's system is solved using the fine mesh contained in the extended domain and the mimetic finite volume method. Next, these local solutions (basis functions) together with a weak continuity condition are used to construct a coarse-mesh version of the global problem that is much cheaper to solve. The basis functions can be used to obtain the fine-mesh details from the solution to the coarse-mesh problem. Our approach leads to a significant reduction in the size of the final system of equations and the computational time, while accurately approximating the behavior of the fine-mesh solutions. We demonstrate the performance of our method using a synthetic 3D example of a mineral deposit.

INTRODUCTION

Electromagnetic (EM) modeling is one of the most important interpretation tools for geophysical exploration. Currently, the two dominant commercial applications of these tools are searching for mineral and petroleum deposits (Oldenburg and Li (2005)). One major challenge in practice is the computational cost involved in the simulation of EM responses of realistic geophysical settings. Such settings often consider highly heterogeneous geologic media and features varying at multiple length scales that may have a significant impact on the behavior of the EM responses of interest. To obtain accurate approximations of the responses in such cases, the mesh used in classical discretization techniques, such as finite volume (FV) or finite element (FE), must capture the structure of the heterogeneity present in the setting with sufficient detail. This leads to the use of very large meshes that translate into solving huge systems of equations.

Adaptive mesh refinement approaches have been used to overcome the computational cost of EM modeling (Horesh and Haber (2011)). Although these approaches have produced accurate approximations to the EM responses at an affordable cost, they face one major issue: the mesh must still capture the spatial distribution of the media heterogeneity both inside and outside the region where we measure the EM responses. This restricts the ability of these approaches to reduce the size of the system to be solved.

Alternatively, multiscale FV/FE techniques aim to reduce the size of the linear system by constructing a coarse-mesh version of the fine-mesh system that is much cheaper to solve. These techniques can be classified within the family of Model Order Reduction methods, where the resulting fine-mesh system from the discretization of the partial differential equation (PDE) is replaced by its projected form. Multiscale FV/FE techniques have been extensively studied in the field of modeling flow in heterogeneous porous media, where they have been successfully used to drastically reduce the size of the linear system while producing accurate solutions. Researchers in this field have noted that the projection matrix constructed using multiscale FV/FE methods may lead to numerical solutions that contain resonance errors. A solution in such cases is to use oversampling techniques in the construction of the projection matrix (Hou and Wu (1997); Jenny et al. (2003); Efendiev and Hou (2009); Hajibeygi and Jenny (2009)). In particular, Haber and Ruthotto (2014) satisfyingly extended multiscale FV techniques for application in EM modeling, where the authors mentioned the need for an oversampling technique to improve the accuracy of the solution obtained with their method for certain cases.

Recognizing the success of oversampling techniques in fluid flow applications, in this paper, we extend their use for application in EM modeling. In particular, we propose an oversampling technique for the multiscale FV method of Haber and Ruthotto (2014) for the quasi-static Maxwell's equations in the frequency domain. We show that our method produces more accurate solutions than the multiscale FV method without oversampling. We demonstrate the performance of our method using a synthetic 3D example of a mineral deposit.

MATHEMATICAL MODEL

The 3D quasi-static Maxwell's equations in the frequency domain subject to non-homogeneous Dirichlet boundary conditions are given by

$$\nabla \times \vec{E} + i\omega\vec{B} = \vec{0}, \quad \text{in } \Omega, \tag{1}$$

$$\nabla \times \mu^{-1}\vec{B} - \Sigma\vec{E} = \vec{s}, \quad \text{in } \Omega, \tag{2}$$

$$\vec{E} \times \vec{n} = \vec{\Phi} \times \vec{n}, \text{ in } \partial\Omega, \tag{3}$$

where $\vec{E}$ is the electric field, $\vec{B}$ is the magnetic flux density, $\vec{s}$ is the source term, ω is the angular frequency, $\vec{n}$ is the unitary outward-pointing normal vector, $\vec{\Phi}$ are given values for the tangential components of $\vec{E}$ due to the boundary conditions, Ω is the domain, and $\partial\Omega$ is the boundary of Ω. The media parameters, μ and Σ, are the magnetic permeability and electrical conductivity, respectively. We assume that these two parameters are 3×3 symmetric positive definite (SPD) tensors. Since the mimetic finite volume (MFV) method is a building block to develop our proposed oversampling technique, we provide an overview of the MFV method. Full details can be found in Haber (2014). MFV is an extension of Yee's method that discretizes highly heterogeneous and anisotropic media in a conservative manner, leading to sparse and symmetric linear systems (Yee, 1966; Hyman and Shashkov, 1999a,b). This method begins by considering the weak form of the system (1)-(2) and uses a staggered mesh to discretizes $\vec{E}$ on the edges, $\vec{B}$ on the faces and the media properties μ and Σ at the cell-centers, yielding the following linear system of equations

$$\mathbf{A}(\boldsymbol{\Sigma})\mathbf{e} = [\mathsf{CURL}^\top \mathbf{M}_f(\boldsymbol{\mu}^{-1})\mathsf{CURL} + i\omega \mathbf{M}_e(\boldsymbol{\Sigma})]\mathbf{e} = -i\omega \mathbf{q}, \tag{4}$$

where $\boldsymbol{\Sigma}$, $\boldsymbol{\mu}$, $\mathbf{e}$, $\mathbf{q}$ are the discrete approximations at the corresponding mesh points for Σ, μ, $\vec{E}$, and $\vec{s}$, respectively. Additionally, CURL, $\mathbf{M}_f(\boldsymbol{\mu}^{-1})$ and $\mathbf{M}_e(\boldsymbol{\Sigma})$ are the corresponding discrete operators for the continuous operator $\nabla\times$ and the mass matrices for the material properties μ and Σ. To impose the boundary conditions, the matrix $\mathbf{A}$ and the vector $\mathbf{e}$ are reordered into interior boundary edges (ie) and boundary edges (be). Thus, the system to be solved in terms of $\mathbf{e}$ is

$$\mathbf{A}_{\mathsf{ie,ie}}\mathbf{e}^{\mathsf{ie}} = -i\omega \mathbf{q}^{\mathsf{ie}} - \mathbf{A}_{\mathsf{ie,be}}\mathbf{e}^{\mathsf{be}}. \tag{5}$$

Once we solved this system, we can compute $\mathbf{b}$ using the discrete version of equation (1).

Multiscale Finite Volume Method with Oversampling: To develop our multiscale method with oversampling (MSFV+O), we adapt the work of Efendiev and Hou (2009) to apply to the multiscale finite volume (MSFV) method for EM modeling proposed by Haber and Ruthotto (2014). Our MSFV+O method can be summarized as follows: (i) we assume a user-chosen coarse mesh nested into a fine mesh, which accurately discretizes the given geophysical setting. Typically the coarse mesh is much smaller than the fine mesh. (ii) For each coarse cell, Ω_k, we independently solve a set of local versions of the source-free Maxwell's system (1)-(2) subject to a set of twelve non-homogeneous Dirichlet linear boundary conditions on an extended domain (one for every edge), Ω_k^{ext}, which includes the coarse cell and a neighborhood of fine cells around it. To solve the twelve local Maxwell's systems, we use the fine mesh contained in the extended domain and the MFV method. We denote the set of discrete solutions as $\mathbf{P}_k^{\mathsf{ext}} = \left[\mathbf{e}_1^{\mathsf{ext}}, \ldots, \mathbf{e}_{12}^{\mathsf{ext}}\right]$. As described in Haber and Ruthotto (2014), this corresponds to a coarse-to-fine local interpolation matrix for the fine-mesh electric field. (iii) Next, these local solutions, called *multiscale basis functions*, coupled with a weak-continuity condition are used to construct a local coarse-to-fine interpolation matrix per coarse cell, $\mathbf{P}_k$. (iv) Once we have computed an interpolation matrix for every coarse cell, we assemble a global interpolation matrix, $\mathbf{P}$, and use it within a Galerkin approach to construct a coarse-mesh version of the fine-mesh system (5) that is much cheaper to solve as follows

$$\mathbf{A}^c(\boldsymbol{\Sigma}^f) = \mathbf{P}^\top \mathbf{A}^f(\boldsymbol{\Sigma}^f)\mathbf{P}, \quad \mathbf{q}^c = \mathbf{P}^\top \mathbf{q}^f. \tag{6}$$

The superscripts c and f denote dependency to the coarse and fine meshes, respectively, and the rest of the terms are defined as before. The basis functions can be used to obtain the fine-mesh details from the solution to the coarse-mesh problem.

The linear boundary conditions imposed to the local Maxwell's problems in step (ii) play a crucial role in accurately capturing the behavior of the EM responses caused by small-scale information of the media present in the problem. If these boundary conditions do not reflect the nature of the underlying heterogeneities, multiscale FV and FE procedures can have large errors. These errors, known as *resonance errors*, appear when the coarse-mesh size and the wavelength of the small scale oscillation of the heterogeneity in the problem we want to solve are close (Hou and Wu (1997); Efendiev and Hou (2009)). By a judicious choice of boundary conditions for the construction of the multiscale basis functions, we can reduce the resonance errors significantly. Oversampling methods are used to reduce boundary effects in the construction of the multiscale basis functions per single coarse-mesh cell. The main idea is to use an extended domain to avoid this boundary effects and to use only the fine-mesh information at the interior of the cell to construct the local basis functions.

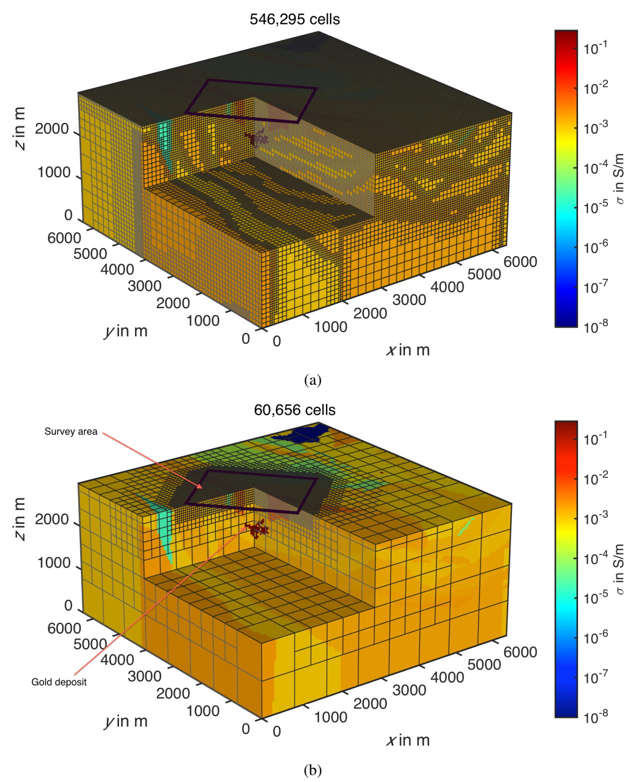

Figure 1: Subsurface of the synthetic electrical conductivity model and setup for our large-loop EM survey. (a) Model discretized on a fine OcTree mesh used to compute a reference solution. (b) Model discretized on a coarse OcTree mesh used to compute multiscaled solutions.

We now proceed to discuss step (iii) in detail, which along with step (ii) form the core idea behind our proposed oversampling strategy. For a given coarse cell Ω_k, this idea consists of computing the local interpolation matrix $\mathbf{P}_k$ from $\mathbf{P}_k^{\mathsf{ext}}$ coupled with a weak continuity condition that enables the use of the new projection matrix within the Galerkin formulation that follows in step (iv). Following Efendiev and Hou (2009), we assume that the set of local basis functions in Ω_k can be expressed as a linear combination of the extended basis functions as follows

$$\mathbf{e}_j(\vec{x}) = [\mathbf{e}_1^{\mathsf{ext}}, \ldots, \mathbf{e}_{12}^{\mathsf{ext}}]\mathbf{c}_j, \quad j = 1, \ldots, 12, \tag{7}$$

where $\mathbf{c}_j$ are coefficients to be determined. In order to uniquely determine such coefficients, we impose the following weak continuity condition given by

$$\mathscr{A}_{\hat{e}_m}(\mathbf{e}_i) := \frac{1}{L_{\hat{e}_m}} \int_{\hat{e}_m} \mathbf{e}_i \cdot \tau_{\hat{e}_m} \, ds = \delta_{mi}, \tag{8}$$

to 7 that yields to the system of equations to determine the coefficients as follows

$$\mathscr{A}_{\hat{e}_j}(\mathbf{e}_1) = \left[\mathscr{A}_{\hat{e}_1}\left(\mathbf{e}_1^{\text{ext}}\right), ..., \mathscr{A}_{\hat{e}_{12}}\left(\mathbf{e}_{12}^{\text{ext}}\right)\right] \mathbf{c}_j, \quad j = 1, ..., 12. \tag{9}$$

Combining equations (9), (8) and (7), we obtain the desired expression for the coefficients

$$\mathbf{C} = \begin{bmatrix} \mathbf{p}_{\hat{e}_1}^\top \mathbf{e}_1^E & \mathbf{p}_{\hat{e}_2}^\top \mathbf{e}_1^E & \cdots & \mathbf{p}_{\hat{e}_{12}}^\top \mathbf{e}_1^E \\ \mathbf{p}_{\hat{e}_1}^\top \mathbf{e}_2^E & \mathbf{p}_{\hat{e}_2}^\top \mathbf{e}_2^E & \cdots & \mathbf{p}_{\hat{e}_{12}}^\top \mathbf{e}_2^E \\ \vdots & \vdots & \ddots & \vdots \\ \mathbf{p}_{\hat{e}_1}^\top \mathbf{e}_{12}^E & \mathbf{p}_{\hat{e}_2}^\top \mathbf{e}_{12}^E & \cdots & \mathbf{p}_{\hat{e}_{12}}^\top \mathbf{e}_{12}^E \end{bmatrix}^{-1}. \tag{10}$$

Finally, we form the local interpolation operator $\mathbf{P_k}$, by computing

$$\mathbf{P}_k = \mathbf{P}_k^{\text{ext}}|_{\Omega_k} \mathbf{C} \tag{11}$$

where $\mathbf{P}_k^{\text{ext}}|_{\Omega_k}$ represents the list of indexes of fine-mesh edges inside the coarse-mesh cell Ω_k.

NUMERICAL RESULTS

In this section, we demonstrate the performance of our proposed oversampling technique for the multiscale finite volume (MSFV+O) method using a synthetic 3D example of a mineral deposit. The results are compared to those obtained using the MFV method on a fine mesh, and the MSFV method (Haber and Ruthotto (2014)) on a coarse mesh. For this example, we construct a synthetic electrical conductivity model based on the inversion results of field measurements over the Canadian Lalor mine obtained by Yang et al. (2014). The conductivity model, shown in Figure 1, has an area with non-flat topography and extends from 0 to 6.5km along the x, y and z directions, respectively. The model comprises air and the subsurface that is composed of 35 geologic units. The unit with the largest conductivity value represents a gold deposit. We assume a conductivity of 10^{-8}S/m in the air. The subsurface conductivity values range from 1.96×10^{-5}S/m to 0.28S/m. In addition, we consider a large-loop EM survey for this example, where we use a rectangular transmitter loop with dimensions 2km×3km, operating at the frequencies of 100, 200 and 400Hz. The transmitter is placed on the Earth's surface and it is centered above the gold deposit (Figure 1). Inside the loop, we place a uniform grid of receivers that measure the three components of the magnetic flux. The receivers are separated by 50m along the x and y directions, respectively. To reduce the effect of the imposed natural boundary conditions (3), we embed the survey area into a much larger computational domain which replaces the true decay of the fields towards infinity (Figure 1).

Our aim is to estimate the secondary magnetic flux induced by the gold deposit in the survey area. For this purpose, we simulate two sets of the magnetic flux data for each frequency. The first data set considers the conductivity model including all geologic units, and the second data set excludes the gold deposit from the original conductivity model. The secondary magnetic flux induced by the gold deposit, denoted as $\Delta\vec{B}$, is then computed by subtracting the two data sets. To compute a reference solution, we discretize our conductivity model at the cell centers of a fine OcTree mesh using the MFV method (Haber (2014)). The fine mesh has cell sizes of $(50\text{m})^3$ within the survey area and at the interfaces of the model where the conductivity varies, the rest of the domain is padded with coarser OcTree cells (Figure 1(a)). This mesh has 546,295 cells. To get an estimate for the proper cell size, we consider the largest background conductivity value (4.5×10^{-3}S/m) and calculate skin depths of 745, 527 and 373m for the 100, 200 and 400Hz frequencies, respectively. We find that using cells of size 50, 100 and 200m is sufficient to capture the decaying nature of the magnetic flux in the survey area. Using the MFV method on the fine OcTree mesh yields systems with roughly 1.5 millions degrees of freedom (DOF) which we solve using the direct solver MUMPS (Amestoy et al. (2001)). The computation time per single simulation is 883s on a two hexa-core Intel Xeon X5660 CPUs at 2.8Hz, 64 GB shared RAM using MATLAB. The real and imaginary parts of the results obtained for the z-component of $\Delta\vec{B}$, denoted as ΔB^z, at 100Hz are shown in Figures 2(a,b).

In order to use the MSFV+O method introduced in the previous section, we need to choose a suitable coarse mesh and the size of the oversampling area to compute the local projection matrix. For the coarse mesh, we consider a coarser OcTree mesh nested in the fine OcTree mesh. The coarser mesh is designed to maintain the fine-mesh resolution $(50\text{m})^3$ inside the survey area, whereas the rest of the domain is filled with increasingly coarser cells (Figure 1(b)). In total, this mesh contains 60,656 cells. To analyze the performance of our MSFV+O method for coarse OcTree meshes, we do not refine the mesh outside the survey area where a large conductivity contrast is present in the model (Figure 1(b)). Next, to investigate the effect of the size of the oversampling area, i.e., the number of fine-mesh padding cells by which we extend every coarse cell on the resulting magnetic flux data, we pad the coarse cell using 2, 4, and 8 fine cells.

Applying the MSFV+O method, we obtain reduced linear systems with 169,892 DOF, which are also solved using MUMPS. The total run times for oversampling sizes of 2, 4 and 8 padding cells are 186, 526 and 3,680s, respectively, on the same machine. The real and imaginary parts of ΔB^z at 100Hz are shown in Figures 2(c,d). We also carry out simulations using the MSFV method (Haber and Ruthotto (2014)) on the coarse OcTree mesh shown in Figure 1(b). We first adapt the MSFV method for OcTree meshes, as the original version is derived for tensor meshes only. This method also yields reduced systems of equations which are solved using MUMPS. The total run time per single simulation is 84s on the same machine. The real and imaginary parts of ΔB^z at 100Hz are shown in Figures 2(e,f).

Table 1 shows the relative errors in infinite norm for the real and imaginary parts of ΔB^z obtained from comparing the reference solution with the MSFV and MSFV+O solutions for each frequency and oversampling size. From this table, we observe the following. First, our oversampling technique significantly improves the accuracy for both the real and imaginary parts of the solution in comparison to the MSFV method as the errors decrease with oversampling. Second, as the oversampling size increases the error decreases at the expense of more computational run time, which, however, is still considerably lower compared to the time of the reference solution for the cases of 2 and 4 padding cells. Third, for a simulation at 400Hz with an oversampling size of 8 padding cells the slight increment in the error of the imaginary part may be caused by excessive coarsening for such high frequency. Four, for the simulation at 200Hz the increase and decrease in the error going from padding cell 2 to 4 and 4 to 8, respectively, may be related to the combined discretization error in simulating secondary field data.

Table of relative errors

Method	Frequency 100Hz	200Hz	400Hz
Relative errors for real part of ΔB^z (%)			
MSFV	69.76	70.30	54.71
MSFV+O (2 pc)	14.61	12.87	8.84
MSFV+O (4 pc)	12.88	11.35	8.39
MSFV+O (8 pc)	10.57	8.52	7.48
Relative errors for imaginary part of ΔB^z (%)			
MSFV	69.17	58.02	73.25
MSFV+O (2 pc)	11.96	23.53	19.11
MSFV+O (4 pc)	10.11	29.47	12.92
MSFV+O (8 pc)	9.95	25.08	14.54

Table 1: Relative errors in infinite norm for the real and imaginary parts of ΔB^z. Note that pc stands for padding cells.

CONCLUSIONS

We develop an oversampling technique for the multiscale finite volume method to simulate electromagnetic responses in the frequency domain for geophysical settings that include highly heterogeneous media. Our method produces results comparable to those obtained by simulating electromagnetic responses on a fine mesh using classical discretization methods, such as mimetic finite volume, while drastically reducing the size of the linear system and the computational time. Using the oversampling technique in the presented example, the size of the coarse-mesh system is only about 10% of the fine-mesh system size, while the relative error is less than 30% for all the cases considered.

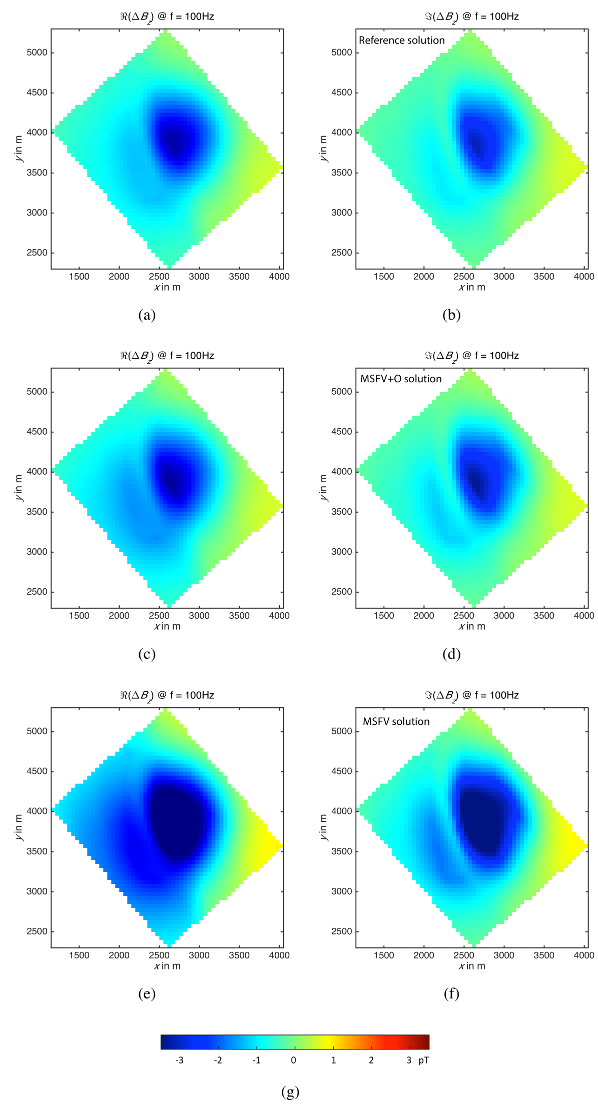

Figure 2: Numerical results for our large-loop EM survey for 100Hz. The first and second columns visualize the real and imaginary parts of the z-component of the secondary magnetic fluxes of the gold deposit, ΔB^z, respectively. Top row: reference solution computed using the MFV method on the fine OcTree mesh with 546,295 cells. Middle and bottom rows: results using the MSFV+O (with 8 padding cells) and MSFV methods on the coarse OcTree mesh with 60,656 cells, respectively. All results are shown in picoteslas (pT) and plotted using the same color scale (g).

EDITED REFERENCES

Note: This reference list is a copyedited version of the reference list submitted by the author. Reference lists for the 2016 SEG Technical Program Expanded Abstracts have been copyedited so that references provided with the online metadata for each paper will achieve a high degree of linking to cited sources that appear on the Web.

REFERENCES

Amestoy, P. R., I. S. Duff, J.-Y. L'Excellent, and J. Koster, 2001, MUMPS: A general purpose distributed memory sparse solver, *in* T. Sorevik, F. Manne, R. Moe, A. H. Gebremedhin, eds., Applied Parallel Computing. New Paradigms for HPC in Industry and Academia: 5th International Workshop, PARA 2000 Bergen, Norway, June 18-20, 2000 Proceedings: Springer, 1–5.

Efendiev, Y., and T. Y. Hou, 2009, Multiscale finite element methods: Theory and applications: Springer.

Haber, E., 2014, Computational methods in geophysical electromagnetics: SIAM.

Haber, E., and L. Ruthotto, 2014, A multiscale finite volume method for Maxwell's equations at low frequencies: Geophysical Journal International, **199**, 1268–1277, http://dx.doi.org/10.1093/gji/ggu268.

Hajibeygi, H., and P. Jenny, 2009, Multiscale finite-volume method for parabolic problems arising from compressible multiphase flow in porous media: Journal of Computational Physics, **228**, 5129–5147, http://dx.doi.org/10.1016/j.jcp.2009.04.017.

Horesh, L., and E. Haber, 2011, A second order discretization of Maxwell's equations in the quasi-static regime on OcTree grids: SIAM Journal on Scientific Computing, **33**, 2805–2819, http://dx.doi.org/10.1137/100798508.

Hou, T. Y., and X.-H. Wu, 1997, A multiscale finite element method for elliptic problems in composite materials and porous media: Journal of Computational Physics, **134**, 169–189, http://dx.doi.org/10.1006/jcph.1997.5682.

Hyman, J. M., and M. Shashkov, 1999a, Mimetic discretizations for Maxwell's equations: Journal of Computational Physics, **151**, 881–909, http://dx.doi.org/10.1006/jcph.1999.6225.

Hyman, J. M., and M. Shashkov, 1999b, The orthogonal decomposition theorems for mimetic finite difference methods: SIAM Journal on Numerical Analysis, **36**, 788–818, http://dx.doi.org/10.1137/S0036142996314044.

Jenny, P., S. H. Lee, and H. A. Tchelepi, 2003, Multi-scale finite-volume method for elliptic problems in subsurface flow simulation: Journal of Computational Physics, **187**, 47–67, http://dx.doi.org/10.1016/S0021-9991(03)00075-5.

Oldenburg, D. W., and Y. Li, 2005, Inversion for applied geophysics: A tutorial, *in* D. K. Butler, ed., Near-surface geophysics: SEG Books, 89–150.

Yang, D., D. Fournier, and D. W. Oldenburg, 2014, 3D Inversion of EM data at Lalor mine: In pursuit of a unified electrical conductivity model: Exploration for Deep VMS Ore Bodies: Hudbay Lalor Case Study, BC Geophysical Society, 1–4.

Yee, K., 1966, Numerical Solution of Initial Boundary Value Problems Involving Maxwells Equations in Isotropic Media: IEEE Transactions on Antennas and Propagation, **14**, 302–307, http://dx.doi.org/10.1109/TAP.1966.1138693.